Processing and Characterization of High-Density Fe-Silicide/Si Core-Shell Quantum Dots for Light Emission

Katsunori Makihara, Yuji Yamamoto, Markus Andreas Schubert, Andreas Mai and Seiichi Miyazaki

Abstract

The monolithic integration of Si–based photonics with electronic processes on a single chip is considered a key advancement for beyond-CMOS computing. However, from an application point of view, Si–based photonics necessitate Si–based light sources that are highly compatible with Si–ULSI processing. In this paper, our achievements on fabrication of Si quantum dots (QDs) with a β–FeSi2 core referred to as super–atom like QDs by controlling self–aligned silicidation of the Si–QDs and subsequent selective Si–growth, and their light emission properties have been reviewed.

To systematically investigate the silicide process and selective Si–growth, SOI substrates were utilized. Initially, the Si layer on the SiO2 was thinned to ~10 nm by alternately controlling the thermal oxidation and wet etching using a diluted HF solution. Subsequently, ~1.0 nm–thick Fe–films were deposited via EB evaporation. The Fe–film was then immediately removed using an HCl solution. Following this, the sample was exposed to SiH4 at 400℃. The formation of the ultrathin Fe–silicide layer and Si growth on the silicide layer was confirmed through cross-sectional TEM–EDX mapping images (Fig. 1). Despite the Fe film being deposited at room temperature and subsequently etched by HCl, the formation of an ultrathin Fe layer was observed. Conversely, Si signals were detected throughout the sample, irrespective of the film thickness direction. It was confirmed that the top surface of the sample was oxidized. Furthermore, the growth of Si on the Fe surface was confirmed by analyzing the atomic concentration of each element in the film thickness direction, as evaluated from the cross–sectional profile, indicating the formation of a sandwich structure in which the Fe–silicide layer was sandwiched between the Si layers. It is noteworthy that the atomic concentration ratio of Fe to Si was close to 1:2, suggesting the formation of the FeSi2–phase.

Based on these results, we applied the same processes as discussed for the SOI substrate, to form a new type of superatom structure, namely, Fe–silicide core/Si–shell QD on an ultrathin SiO2 layer (Fig. 2). First, uniformly sized Si–QDs with an areal density as high as ~1011cm-2 were self–assembled on a ~3.0 nm thick SiO2 layer/p–Si (100) by precisely controlling the LPCVD using SiH4 gas, where the average dot height calculated using a log–normal fitting function was estimated to be ~5.1 nm. After the ~1.0 nm thick Fe–film deposition, the surface morphology was slightly smeared, and the average dot height slightly decreased to ~3.9 nm. However, after the HCl treatment, the dot height became the same size, which was ~5.1 nm as that of the as-grown Si–QDs. Subsequent SiH4 exposure at 400°C, resulted in a slight increase up to ~5.9 nm with no change in the areal dot density. We also confirmed that no Si–deposition occurred on the SiO2 surface at 400°C because the decomposition temperature of SiH4 was not reached. Considering the results of the SOI discussed earlier, these results are expected to form β–FeSi2 core/Si–Shell QDs. This indicates that the silicidation reaction of the Si–QDs surface occurred immediately after Fe film deposition. Subsequently, the unreactive Fe films were etched by the HCl treatment. Followed by SiH4 exposure, Si was selectively grown on the Fe silicide surface, acting as an outer cladding. To clarify the crystalline phase of the silicide core, we measured the room–temperature PL, using a semiconductor laser with a wavelength of 976 nm at an input power of ~0.33 W/cm2 as an excitation source (Fig. 3). Although a weak PL signal in the range from ~0.73 to 0.83 eV was observed immediately after the Fe deposition, light emission from the sample was hardly detected after HCl treatment. These results can be explained as follows: immediately after the Fe–film deposition, β–FeSi2 layer was formed on the Si–QDs surface despite the oxidation. Conversely, after HCl treatment, non–radiative recombination centers at the β–FeSi2 surface dominated due to the complete etching of the surface oxide. It is noteworthy that after SiH4 exposure, PL intensity with no significant change in wavelength was observed, and the PL intensity drastically increased by a factor of five compared to that after Fe film deposition. This result provides clear evidence for the formation of core/shell dots, indicating that the ultrathin Si cap layer was conformally covered with the dots, resulting in the suppression of defects on the β–FeSi2 surface.

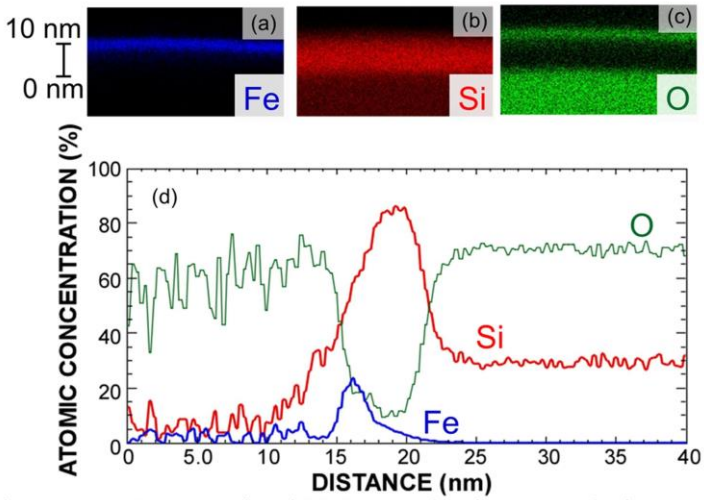

Fig. 1 (a–c) Cross–sectional EDX mapping images and (d) cross–sectional profile of the sample corresponding to Fig. 1d, in the EDX mapping images, the blue, red, and green colors correspond to Fe, Si, and O, respectively.

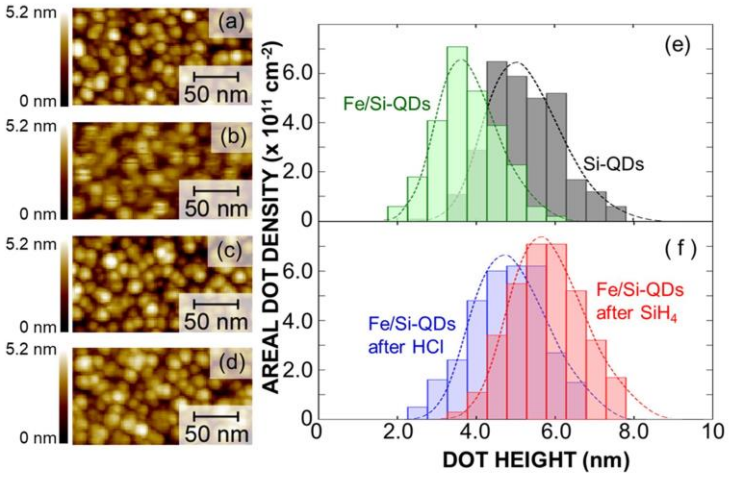

Fig. 2 (a–d) Typical AFM images, (e, f) dot height distribution evaluated from the AFM images of (a) pre–grown Si–QDs, (b) after Fe–film deposition, (c) after HCl treatment, and (d) subsequent SiH_4 exposure, wherein the dot height distribution.

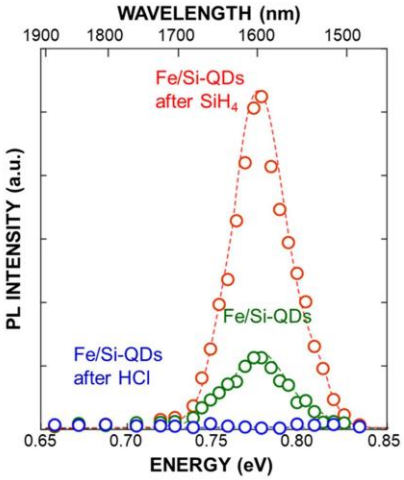

Fig. 3. PL spectra of the NDs.

Figure 1